

**NASA Technical Memorandum 83297**

NASA-TM-83297 19820015321

STATIC AND UNSTEADY PRESSURE MEASUREMENTS  
ON A 50 DEGREE CLIPPED DELTA WING AT  $M = 0.9$

R. W. HESS, E. C. WYNNE, AND F. W. CAZIER, JR.

APRIL 1982

**LIBRARY COPY**

APR 16 1982

LANGLEY RESEARCH CENTER  
LIBRARY, NASA  
HAMPTON, VIRGINIA

**NASA**

National Aeronautics and  
Space Administration

**Langley Research Center**  
Hampton, Virginia 23665



STATIC AND UNSTEADY PRESSURE MEASUREMENTS ON A 50 DEGREE  
CLIPPED DELTA WING AT  $M = 0.9$

R. W. Hess, E. C. Wynne, and F. W. Cazier  
NASA Langley Research Center  
Hampton, Virginia 23665

Abstract

Static and unsteady pressures were measured on a 50.45 degree clipped delta wing in the Langley Transonic Dynamics Tunnel with Freon as the test medium. Data taken at  $M = 0.9$  is presented for static and oscillatory deflections of the trailing edge control surface and for the wing in pitch. Comparisons of the static measured data are made with results computed using the Bailey-Ballhaus small disturbance code.

Nomenclature

b	half mean chord length, m
c	local chord length, m
$C_{pu}$	upper surface pressure coefficient, static or dynamic modulus
f	frequency
k	$\frac{b\omega}{V}$ , reduced frequency
M	Mach number
q	dynamic pressure, kPa
t/c	thickness ratio
V	free stream velocity, m/s
$\frac{x}{c}$	fraction of chord
$\alpha$	peak oscillation amplitude in pitch, deg.
$\bar{\alpha}$	mean angle of attack or static angle of attack, degrees
$\Delta C_p$	lifting pressure coefficient, $C_{pL} - C_{pu}$ , static or dynamic modulus
$\delta$	peak oscillation amplitude of control surface, deg.
$\bar{\delta}$	control surface static angle, positive trailing edge down, deg
n	fraction of semi span
$\phi$	velocity potential
$\phi$	phase, angle, deg.

Introduction

The prediction of unsteady aerodynamic forces on oscillating airfoils and controls at transonic speeds has been the subject of experimental and computational studies for many years, for example, Lambourne (ref. 1) and Lessing, Troutman and Menees (ref. 2). In the past few years there has been a significant effort

spent to develop an experimental data base for verification of transonic computer codes and to improve understanding of the complex flow phenomena at transonic speeds. Notable examples of these efforts are Tijdeman and Davis (ref. 3 and 4) with two dimensional airfoil studies and Sandford, et al (ref. 5) with a high aspect ratio wing with multiple leading and trailing edge control surfaces. The present paper contains some results from an experimental study of static and oscillating pressures measured on a clipped delta wing. The pressures were generated by deflections of the trailing edge control surface and deflections of the wing in pitch. Static pressure comparisons are made between the measured data and calculated pressure from the Bailey-Ballhaus small disturbance code (ref. 6).

Description of Apparatus

Wing

The pertinent configuration parameters of the wing are given in the sketch in Figure 1. The clipped delta, semi-span, wing had a sweep angle of 50.45 degrees, a panel aspect ratio of 1.242, and a circular arc airfoil with a 6 percent thickness ratio. The semi-span is 1.143 meters and the root chord is 1.614 meters. The pitch axis is located at 65.22 percent of the root chord. At the first wing resonant frequency, 28 Hz, there are significant dynamic bending deflections outboard of the control surface which restricted the maximum excitation frequency to 22 Hz.

The wing was constructed of stainless steel ribs and spars with a Kevlar-epoxy skin and weighed 53.93 kilograms. The trailing edge control surface, ribs and skin, is a graphite epoxy structure built around a step-tapered steel shaft. For this test a dummy leading edge control was substituted for the movable control.

Wing Mounting and Oscillation System

The wing was mounted on a hydraulically driven oscillating drive system on the side wall of the Langley Transonic Dynamics Tunnel as shown in Figure 2. It is supported on a tapered shaft of the drive system that mates to a tight fitting cavity in the wing. A wing fence at the root of the wing was designed to seal the wing at the juncture with a splitter plate. The splitter plate was constructed in two sections, a rigid outer section, and a remotely controlled, compliant center section that fits over the wing fence and permits oscillation about a variable mean angle of attack. The wing static position and the dynamic amplitude are under control of two separate systems; the first is electro-mechanical and the second hydraulic. The dynamic system was designed to be operated as a spring-mass system at a resonance condition in pitching using heavy tuned springs.

Previous experience with inexorably driven airfoils had indicated that a spring-mass system would be desirable in that it would result in a lighter loading on the drive mechanism. In practice the springs were tuned to only one stiffness and the system was operated at off-resonant frequencies such that a tunnel entry was not made for each change in frequency. It was also necessary to preload the springs to one degree deflection to eliminate load reversal in the system through the range of oscillation amplitude. The separate hydraulic systems which drive the wing in oscillation and control surface position, static and dynamic, are controlled by servo feedback systems.

### Instrumentation

The wing was instrumented with 76 dynamic pressure transducers and 81 static orifices. The location of the upper surface transducers and static orifices are given in Tables 1-a and 1-b. There were nine accelerometers mounted in the wing at the locations given in Table 2. The accelerometers were installed to measure the dynamic amplitude including the effects of deflection due to out of plane dynamic deformation. The control surface deflection and the model mean angle of attack were measured with potentiometers. The wing oscillation amplitude was measured with a linear variable differential transformer. Strain gage bridges on the wing structure and in the control surface shaft measured strain and moments for loads monitoring purposes.

### Test Conditions

The wing was tested in the Langley Transonic Dynamics Tunnel in Freon at a dynamic pressure,  $q$ , of 9.34 kPa (195 psf) and at a Reynolds number of  $10 \times 10^6$  based on the mean chord length of 0.922 meters. Boundary layer transition strips were fixed on the wing surface at 8 percent chord from the leading edge. The grit size varied from number 70 at the root to number 90 at the tip.

### Data Reduction

The static and dynamic data were digitally recorded at the rate of approximately 950 samples per second per channel. Data acquisition and display were under control of the facility computer (ref. 7) and the daily post-test data processing and analysis were performed on this system. The static data were converted to engineering units and analyzed during the test. However, the dynamic data were analyzed post-test to determine the Fourier coefficients from which the modulus and phase were determined. The reduced static and dynamic data sets were then put on file at the Langley central computer facility for further examination and analysis.

The symmetry of the airfoil section permitted use of the top surface transducers and static orifices to measure pressure differentials. The top surface pressures were measured at a positive angle of attack and the lower surface pressures were obtained as the upper surface pressures measured at a negative angle

of attack. The surface distribution of  $\Delta C_p$ , static and dynamic, was computed from the two relevant sets of data on the central computer.

### Static Calculations

Static pressure distributions for pitch and control surface deflections were computed using the modified three-dimensional, transonic small disturbance, Bailey-Bailhaus code. A conservative difference method is used except for the cross term  $\phi_{xy}$ . This code (ref. 6) has options for a viscous boundary layer and the Murman bump, an empirical method for modeling shock-boundary layer interaction. Both the boundary layer and bump options gave essentially the same pressure distributions and shock location using the standard default options. However, the inviscid option, which was used in the present paper, gave the best comparison with experiment in that the shock location is further aft and in better agreement with experiment. The calculated pressure distributions for the deflected control surface were made by dividing the wing spanwise into three panels and changing the local airfoil coordinates at the control surface location for each deflection angle.

### Results and Discussion

As an introduction to the results, a calculated static pressure distribution of the upper surface at a wing angle of attack ( $\bar{\alpha}$ ) of two degrees is shown in Figure 4. Changes in the chordwise pressure distribution with span is evident. These characteristics appear in succeeding static and unsteady results.

### Static Results

The experimental and calculated variations of  $C_{p_u}$  (upper surface pressure) and  $\Delta C_p$  (lifting pressure) with chord position are shown in figures 5 and 6 for pressures induced by wing pitch and control surface deflection.

The variation of static pressure with angle of attack (Fig. 5a, 5b) is shown for the five chords. The symbols are the experimental results for angles of attack ( $\bar{\alpha}$ ) of 0, 1, 2, 3, 4 and 4.5 degrees in Fig. 5a for  $C_{p_u}$  and 1, 2, 3, 4, and 4.5 degrees for  $\Delta C_p$  in Fig. 5b, and the lines are the modified Bailey-Bailhaus results for  $\bar{\alpha}$  up to 4 degrees. Agreement between the experimental and calculated results is good for the lower values of  $\bar{\alpha}$  but deteriorates above  $\bar{\alpha} = 2$  degrees. The theory assumes attached flow whereas experimentally the flow separates at the sharp leading edge for  $\bar{\alpha} > 2$  degrees. A vortex is formed that promotes flow reattachment at  $\bar{\alpha} = 3$  degrees at station  $\eta = 0.698$  which expands to the other stations as  $\bar{\alpha}$  is increased.

The data for static deflection of the control surface are given in Fig. 6a and 6b. The upper surface pressure,  $C_{p_u}$ , is presented in Figure 6a for  $\bar{\alpha} = 0$  and control surface deflection angles,  $\bar{\delta}$ , of 0, 2, 4 and 6 degrees. In Figure 6b  $\Delta C_p$  for  $\bar{\alpha} = 2^\circ$  and for  $\bar{\delta} = 0$ ,

2, 6, -2, and -6 degrees are presented. The agreement between experiment and analysis is reasonable for small values of  $\delta$  (2 degrees). However, at large deflection,  $\delta = 6$  deg, the analysis predicts more negative and larger  $\Delta C_p$  pressures than were measured in the neighborhood of the hinge line. It appears that  $\delta = 6^\circ$  is beyond the limits of the small disturbance code for this configuration. It may be noted, however, that the code was very robust and there was little difficulty in obtaining results even for these large deflection angles.

The agreement between the experimental and analytical results for variation in  $\bar{\alpha}$  and  $\delta$  is best at the inboard stations, it decreases with increasing span station. This is most apparent in the results for  $C_{p_u}$  for both sets of data.

#### Unsteady Pressure Measurements

Unsteady first harmonic pressure distributions measured during wing pitching oscillations and for control surface oscillations are given in Figures 7 and 8, respectively. Data are shown for the wing at three mean angles of attack (0 degrees, 2 degrees and 4 degrees) in the form of modulus, and phase angle on the five chords. At  $\bar{\alpha} = 0$  degrees the pressure data is given as  $C_{p_u}$  and at  $\bar{\alpha} > 0$  the results are shown for the lifting pressure,  $\Delta C_p$ . The phase angle between the pressure and its relevant deflection is generally modified by adding or subtracting  $360^\circ$  to present the angle between  $\pm 180$  degrees. Also, a phase difference of  $180$  degrees and a factor of 2 in magnitude between the  $C_{p_u}$  data and the  $\Delta C_p$  data may be noted when comparing the two sets of data. The shift is due to the vector subtraction  $\Delta C_p = C_{p_L} - C_{p_u}$ .

Pitching Oscillations. - The pressure modulus and phase angle resulting from oscillation of the wing in pitch at an amplitude of  $\pm 0.5$  degrees and at a wing mean deflection of 0 degrees, 2 degrees and 4 degrees are given in Figure 7a, 7b and 7c, respectively. The pressure from the shock is apparent in Fig. 7a and 7b,  $\bar{\alpha} = 0$  degrees and 2 degrees, only at a frequency of 16 Hz and is located at an  $x/c$  of 80 percent at  $\eta = 0.337$  and at an  $x/c$  of 60 percent at  $\eta = 0.856$ . At the lower frequency,  $f = 4$  Hz, the modulus actually decreases in the neighborhood of the shock. The dominant feature of the  $\bar{\alpha} = 4$  degree data (Fig. 7c) is the rise in the modulus of the oscillatory lifting pressure,  $\Delta C_p$ , at the leading edge due to the flow separation. The pressure peak due to the shock wave does not appear except at the two outboard stations. The phase distribution in this data shows more variation than the modulus and is similar for all mean angles of attack. The phase angle is  $180^\circ$  at the leading edge for the  $C_{p_u}$  data ( $\bar{\alpha} = 0^\circ$ ) and  $0^\circ$  at the leading edge for the  $\Delta C_p$  data ( $\bar{\alpha} = 2^\circ, 4^\circ$ ), back to the shock location where it increases rapidly. The phase distribution for the 4 degree data differs from the  $\bar{\alpha} = 2$  degrees data in that the phase is negative at the leading edge in the region of the flow separation. The phase angle behind the shock location is always larger for the 4 Hz data.

Control surface oscillations. - Figures 8a, 8b, and 8c give unsteady pressure results due to

control surface oscillation for several values of amplitude,  $\delta$ , and frequency,  $f$ , for static wing angles of attack,  $\bar{\alpha}$ , of 0, 2, and 4 degrees. There are no pronounced effects on the modulus of the lifting pressure,  $\Delta C_p$ , due to frequency of the control surface in the two sets of data. The apparent difference due to changes in  $\delta$  in Figure 8 would be reduced if the data were normalized by the deflection amplitude  $\delta$ . At the higher angle of attack ( $\bar{\alpha} = 4^\circ$ , Fig. 8c) there is a shift in the modulus peak with frequency in the two outboard chords. At the lower frequency,  $f = 8$  Hz, the peak is close to the shock location while at  $f = 22$  Hz the modulus peak moves aft. In contrast to the pitch data, fig. 7c, there is a distinct difference in the phase angle for the two frequencies. The angle is the same only at the trailing edge and on the control surface. Going forward, trailing edge to leading edge, the pressure ultimately lags the deflection by approximately  $180$  degrees for the 8Hz data and by more than  $300$  degrees on the two outboard chords for the 22 Hz data.

#### Concluding Remarks

Some static and oscillatory pressure results are given for a small range of parameters at 0.9 Mach number for a clipped delta wing with a circular arc airfoil.

Calculated results from the Bailey-Ballhaus code compared well with the static experimental data for deflections of the wing or control surface less than 2 degrees. At higher angle of attack flow separation at the wing leading edge precluded satisfactory comparison for the wing in pitch.

The dominant features of the oscillatory wing pitch results are the effects in the pressure induced by the shock wave at the low angles of attack,  $\bar{\alpha} = 2^\circ$ , and the higher lifting pressure modulus due to flow separation at  $\bar{\alpha} = 4$  degrees. The magnitude of the phase shift due to flow separation and reattachment was small, but detectable, in comparison with the shock induced phase shift on the aft portion of the wing. The effects of varying frequency and amplitude on phase were small.

The effects of oscillatory control surface deflection or frequency on the modulus of the lifting pressure were small whereas, in contrast to the pitch data, there is a large phase shift due to change in frequency.

#### References

- 1Lambourne, N. C.: Some Instabilities Arising from Reinteraction Between Shock Waves and Boundary Layers. AGARD Report 182, April 1958.
- 2Lessing, H. C.; Troutman, J. L.; and Menees, G. P.: Experimental Determination of The Pressure Distribution on a Rectangular Wing Oscillating in the First Bending Mode for Mach Numbers From 0.24 to 1.30. NASA TN D-344, Dec. 1960.

<sup>3</sup>Tijdeman, H.: Investigation of the Transonic Flow Around Oscillating Airfoils. NLR-77090-0, 1977.

<sup>4</sup>Davis, S. D.; and Malcolm, G. N.: Experimental Unsteady Aerodynamic of Conventional and Supercritical Airfoils. NASA TM 81221, August 1980.

<sup>5</sup>Sandford, M. C.; Ricketts, R. H.; Cazier, F. W., Jr. and Cunningham, H. J.: Transonic Unsteady Airloads on an Energy Efficient Transport Wing with Oscillating Control Surface. Journal of Aircraft. Vol. 18, No. 7, July 1981.

<sup>6</sup>Mason, W. H.; Ballhaus, W. F.; Mackenzie, C.; Frick, J. and Stern, M.: An Automated Procedure for Computing the Three-Dimensional Transonic Flow Over Wing-Body Combinations, Including Viscous Effects. AFFDL-TR-77-122.

<sup>7</sup>Cole, P. H.: Wind Tunnel Real-Time Data Acquisition System, NASA TM-80081, April 1979.

TABLE 1-a  
Dynamic Orifice Locations  
x/c

Chord	1	2	3	4	5
	.073	.068	.077	.075	.196
	.122	.122	.127	.124	.246
	.197	.249	.199	.198	.345
	.248	.300	.780	.250	.452
	.299	.348	.851	.300	.550
	.349	.449	.901	.348	.603
	.448	.500	.951	.450	.655
	.551	.550		.497	.705
	.601	.601		.548	.781
	.650	.649		.601	
	.698	.700		.651	
	.781	.775		.70	
	.850	.896		.780	
	.900			.903	
				.952	
C,m	1.1474	0.8588	0.7971	0.6470	0.4292
n	33.7	54.55	59.00	69.84	85.57

TABLE 1-b  
Static Orifice Location  
x/c

Chord	1	2	3	4	5
	.078	.069	.082	.068	.207
	.126	.128	.132	.115	.256
	.202	.253	.210	.198	.302
	.252	.304	.788	.256	.354
	.302	.351	.852	.304	.458
	.351	.453	.902	.355	.556
	.451	.504	.951	.454	.607
	.552	.553		.503	.658
	.603	.604		.553	.707
	.652	.653		.604	.798
	.699	.703		.654	
	.781	.769		.703	
	.851	.897		.775	
	.900			.858	
	.950			.904	
				.953	
C,m	1.1536	0.8649	0.8015	0.6535	0.4351
n	33.26	54.11	58.69	69.37	85.14

TABLE 2  
Accelerometer Coordinates

Acc	x/c	n	c,m
1	.2738	.0307	1.5724
2	.2727	.4038	1.0549
3	.7012	.4032	1.0558
4	.2724	.6014	0.7813
5	.7020	.6018	0.7808
6	.2739	.7213	0.6153
7	.7036	.7193	0.6181
8	.2847	.8905	0.3810
9	.7067	.8913	0.3799

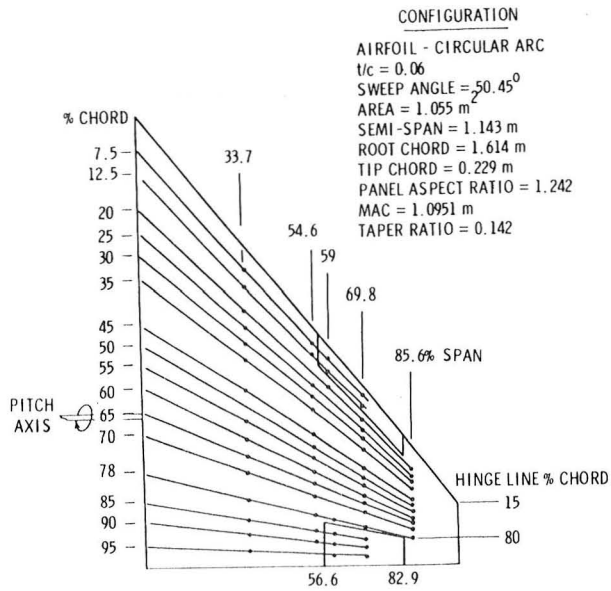


Fig. 1 Clipped Delta Wing

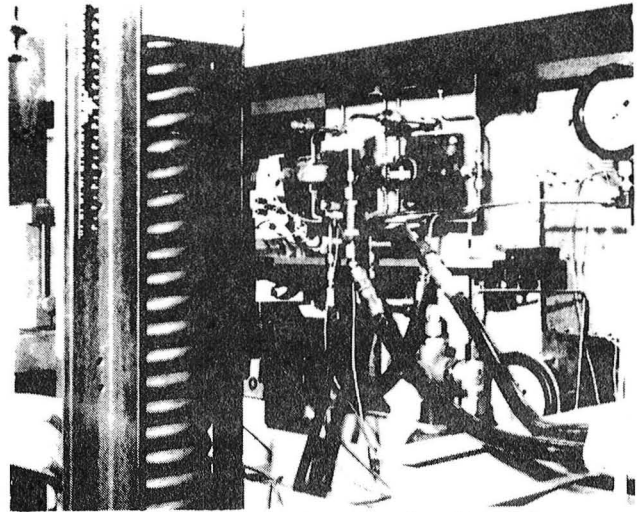


Fig. 3 Model support and hydraulic drive system.

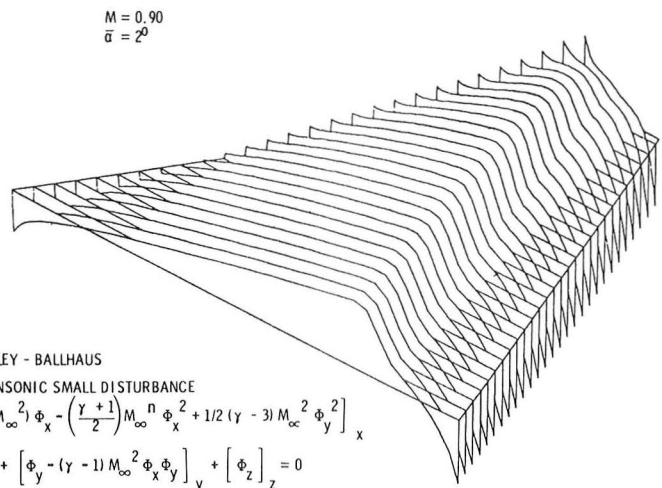


Fig. 4 Upper surface pressure distribution.

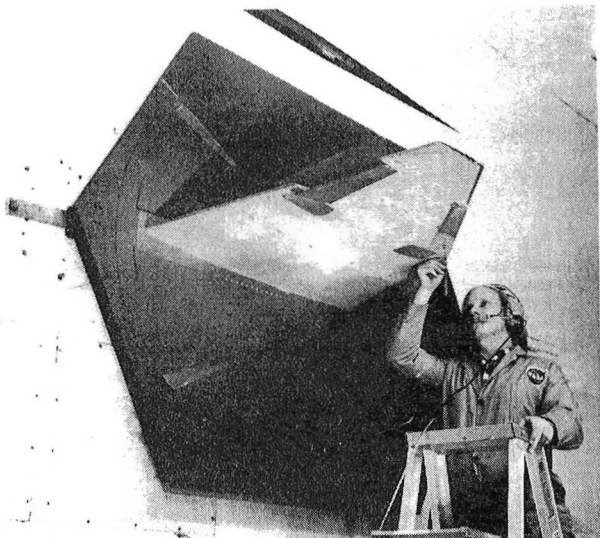


Fig. 2 Model and splitter plate mounted on side wall in TDT.

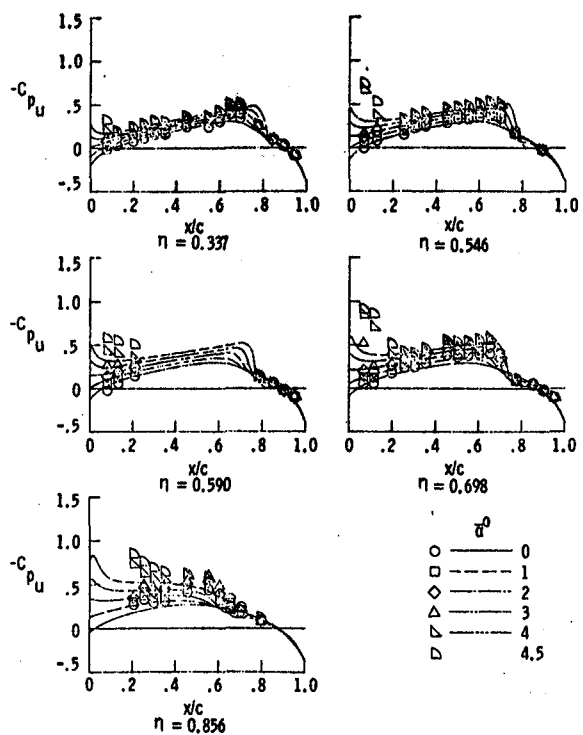


Fig. 5a Variation of static  $C_{p_u}$  with angle of attack at  $M = 0.9$ .

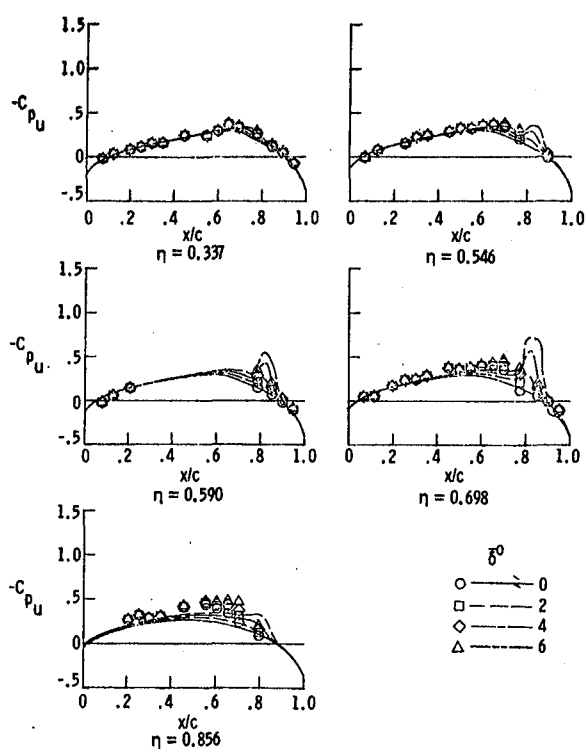


Fig. 6a Variation of static  $C_{p_u}$  with positive control surface deflection at  $\bar{\alpha} = 0$ ,  $M = 0.9$ .

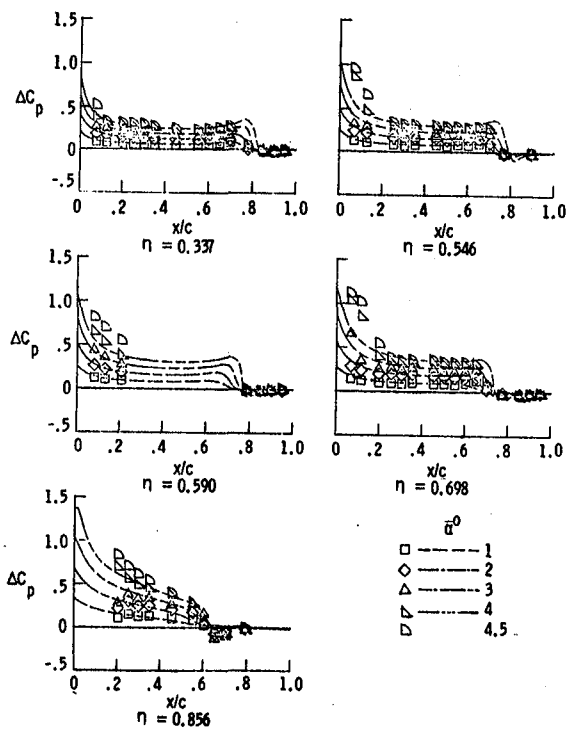


Fig. 5b Variation of static  $\Delta C_p$  with angle of attack at  $M = 0.9$ .

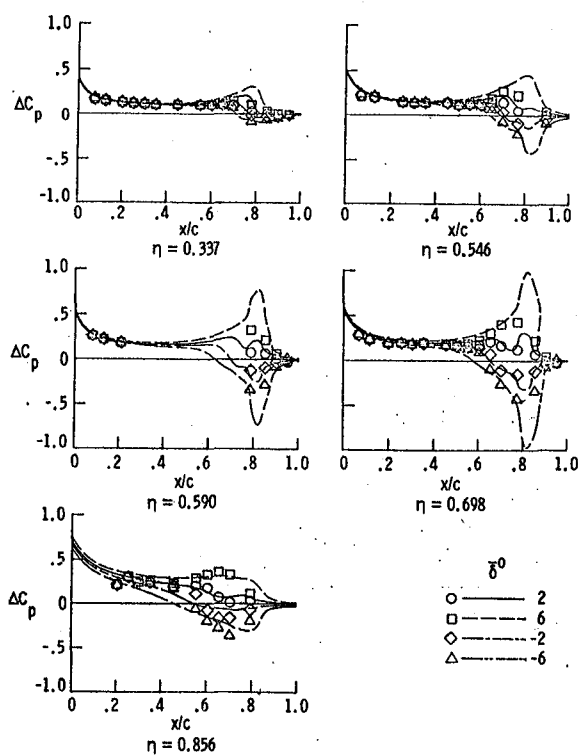


Fig. 6b Variation of static  $\Delta C_p$  with control surface deflection at  $\bar{\alpha} = 2$  deg.,  $M = 0.9$ .



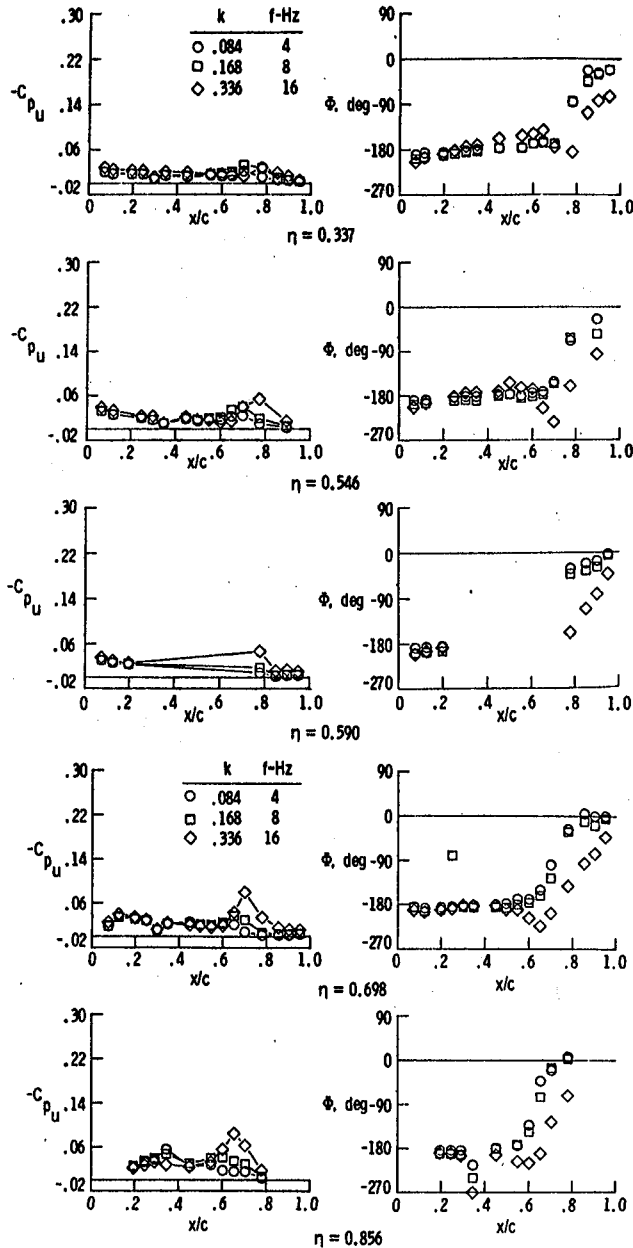


Fig. 7a Modulus of surface pressure,  $C_{p_u}$ , and phase for wing oscillation in pitch at  $\pm 0.5$  deg.,  $\bar{\alpha} = 0$ ,  $M = 0.9$ .

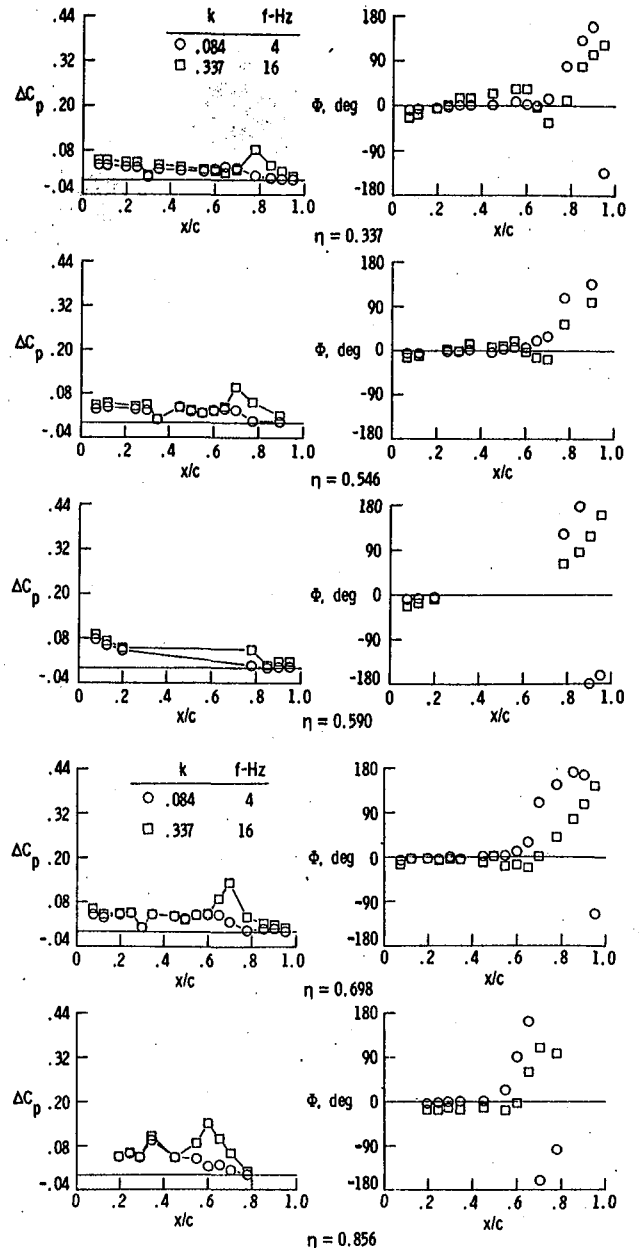


Fig. 7b Modulus ( $\Delta C_p$ ) and phase for wing oscillation in pitch at  $\pm 0.5$  deg.,  $\bar{\alpha} = 2^\circ$ ,  $M = 0.9$ .

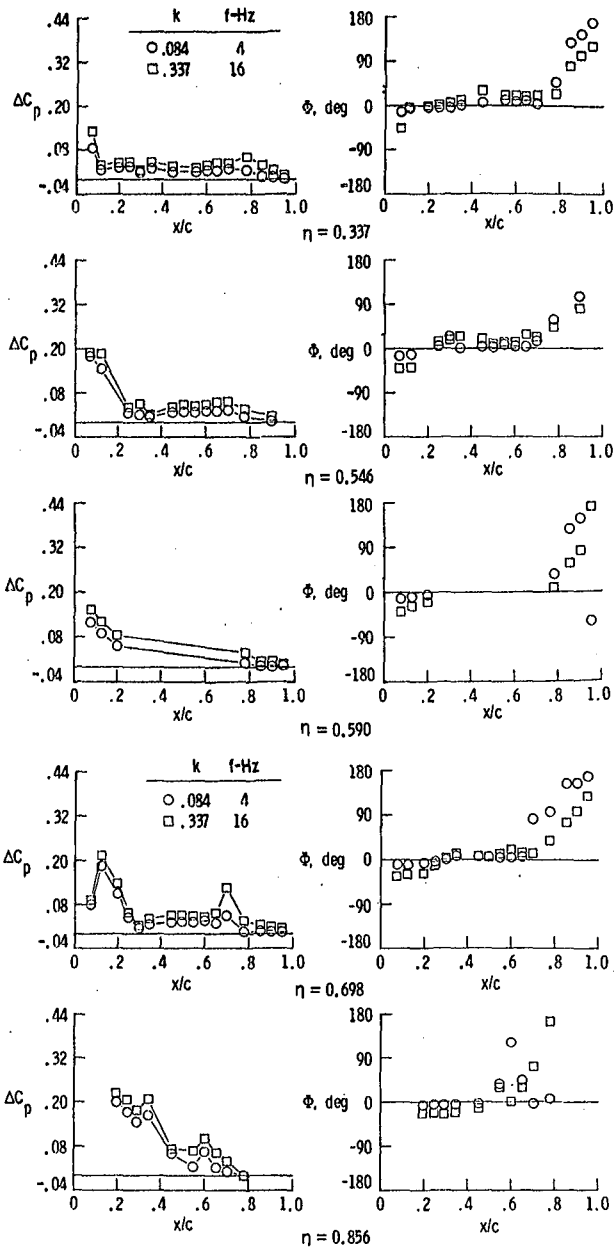


Fig. 7c Modulus ( $\Delta C_p$ ) and phase for wing oscillation in pitch at  $\pm 0.5$  deg.,  $\bar{\alpha} = 4^\circ$ ,  $M = 0.9$ .

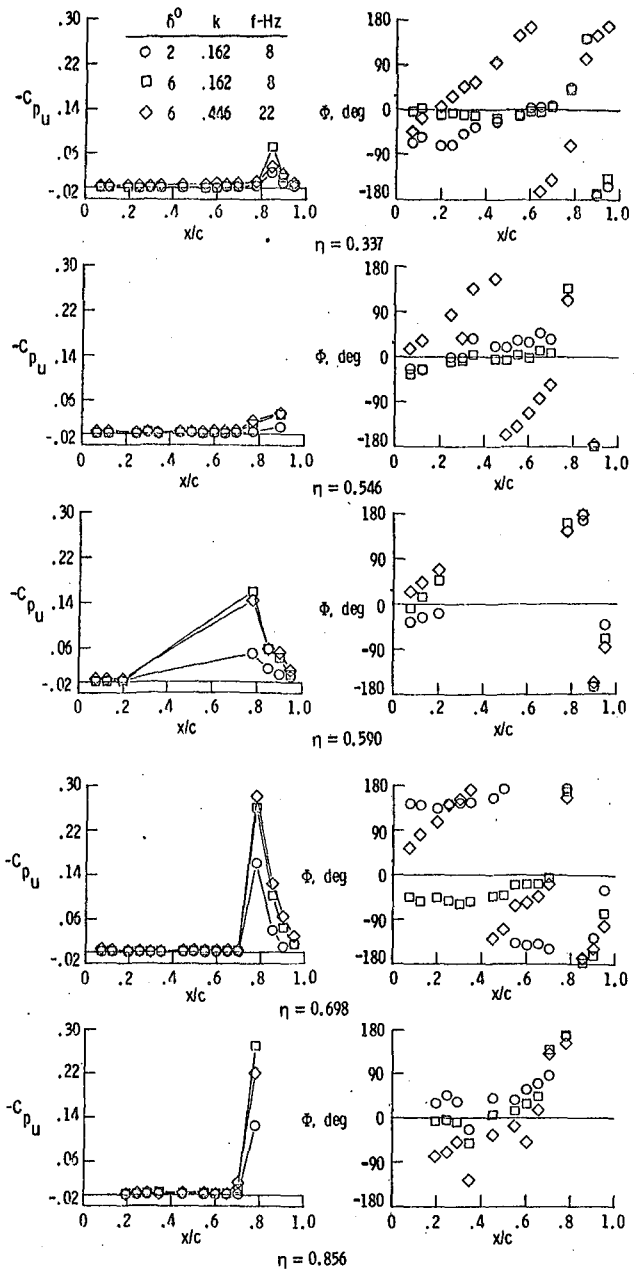


Fig. 8a Modulus of surface pressure,  $C_{p_u}$ , and phase due to control surface oscillation,  $\bar{\alpha} = 0^\circ$ ,  $M = 0.9$ .

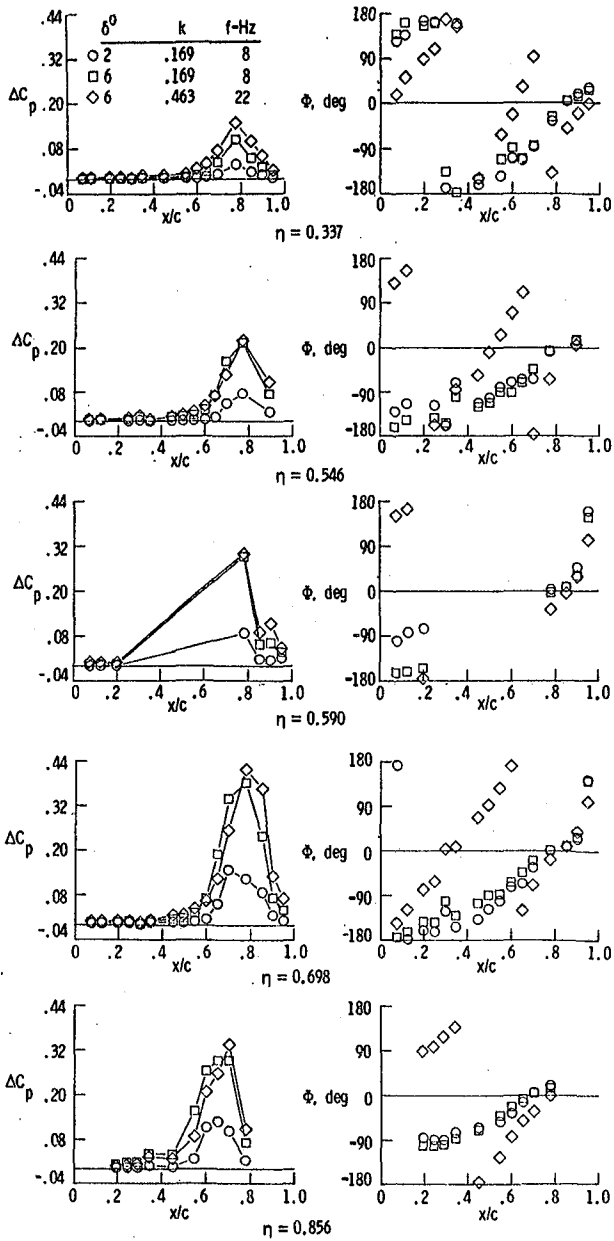


Fig. 8b Modulus ( $\Delta C_p$ ) and phase due to control surface oscillation,  $\bar{\alpha} = 2^\circ$ ,  $M = 0.9$ .

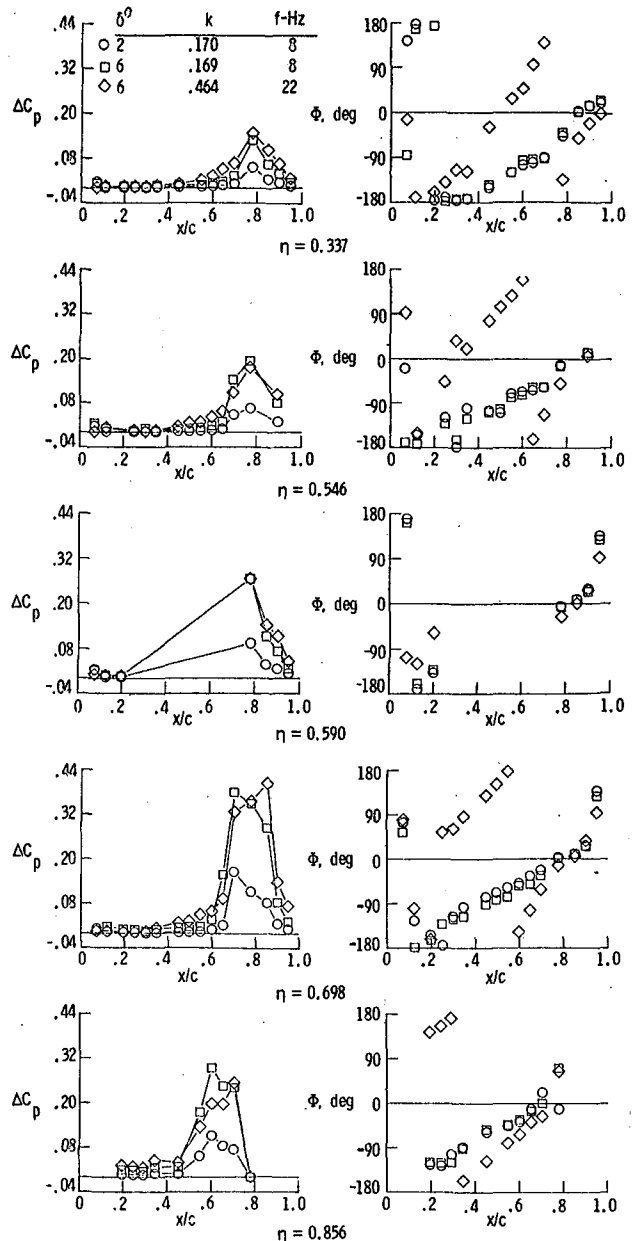


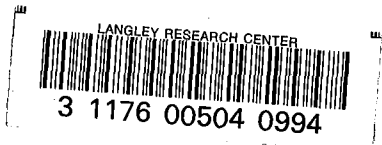
Fig. 8c Modulus ( $\Delta C_p$ ) and phase due to control surface oscillation,  $\bar{\alpha} = 4^\circ$ ,  $M = 0.9$ .





1. Report No. NASA TM 83297		2. Government Accession No.		3. Recipient's Catalog No.	
4. Title and Subtitle STATIC AND UNSTEADY PRESSURE MEASUREMENTS ON A 50 DEGREE CLIPPED DELTA WING AT M = 0.9				5. Report Date April 1982	
				6. Performing Organization Code 2250	
7. Author(s) R. W. Hess, E. C. Wynne, and F. W. Cazier, Jr.				8. Performing Organization Report No.	
9. Performing Organization Name and Address NASA Langley Research Center Hampton, VA 23665				10. Work Unit No. 505-33-53-07	
				11. Contract or Grant No.	
				13. Type of Report and Period Covered Technical Memorandum	
12. Sponsoring Agency Name and Address National Aeronautics and Space Administration Washington, DC 20546				14. Sponsoring Agency Code	
15. Supplementary Notes This paper was presented at the AIAA/ASME/ASCE/AHS 23rd Structures, Structural Dynamics and Materials Conference, May 10-12, 1982, New Orleans, Louisiana, AIAA Paper No. 82-0686.					
16. Abstract Static and unsteady pressures were measured on a 50.45 degree clipped delta wing in the Langley Transonic Dynamics Tunnel with Freon as the test medium. Data taken at M = 0.9 is presented for static and oscillatory deflections of the trailing edge control surface and for the wing in pitch. Comparisons of the static measured data are made with results computed using the Bailey-Ballhaus small disturbance code.					
17. Key Words (Suggested by Author(s)) Measured Unsteady Pressures Measured and Calculated Static Pressures Clipped Delta Wing M = 0.9				18. Distribution Statement Unclassified - Unlimited Subject Category 02	
19. Security Classif. (of this report) Unclassified		20. Security Classif. (of this page) Unclassified		21. No. of Pages 10	22. Price A01





LIBRARY MATERIAL SLIP		
DO NOT REMOVE SLIP FROM MATERIAL		
Delete your name from this slip when returning material to the library.		
NAME	DATE	MS
Kelley Donald	5/1/2008	340